A NOVEL APPROACH TO INCREASE AMPEROMETRIC BIOSENSORS RESPONSE

Rajeev Kumar Ranjan

A NOVEL APPROACH TO INCREASE AMPEROMETRIC BIOSENSORS RESPONSE

Thesis submitted to the
National Institute of Technology, Rourkela
for the award of the degree

of

Master's of Technology in Biomedical Engineering

by

Rajeev Kumar Ranjan

Under the guidance of

Dr. Amitesh Kumar

DEPARTMENT OF BIOTECHNOLOGY & MEDICAL ENGINEERING

NATIONAL INSTITUTE OF TECHNOLOGY, ROURKELA

MAY 2013

CERTIFICATE

This is to certify that the thesis entitled **A novel approach to increase biosensors response**, submitted by **Rajeev Kumar Ranjan** to National Institute of Technology, Rourkela, is an authentic record of bona fide research work carried under my supervision and I consider it worthy of consideration for the award of the degree of Master's of Technology of the Institute.

Date :

Dr. Amitesh Kumar
Assisstant Professor
Department of Biotechnology & Medical Engineering
National Institute of Technology
Rourkela, 769008

DECLARATION

I certify that

1. The work contained in the thesis is original and has been done by myself under the general supervision of my supervisor.
2. The work has not been submitted to any other Institute for any degree or diploma.
3. I have followed the guidelines provided by the Institute in writing the thesis.
4. Whenever I have used materials (data, theoretical analysis, and text) from other sources, I have given due credit to them by citing them in the text of the thesis and giving their details in the references.

Rajeev Kumar Ranjan

CURRICULUM VITA

Name: Rajeev Kumar Ranjan

Educational Qualification:

Year	Degree	Subject	University
2010	BE	Instrumentaion	Pune

ACKNOWLEDGEMENTS

First and foremost, I would like to state my deepest gratitude to my supervisor Dr. Amitesh Kumar, Assistant Professor, Biotechnology and Biomedical Engineering, National Institute of Technology Rourkela for firstly the opportunity to undertake this project and secondly for their guidance, patience and support throughout my study. They have always pointed me in the right direction with their experience and their contributions to this research are greatly appreciated. He has consistently pushed me to deliver my best, and I am very grateful to him for supervising me throughout the year. I am grateful to the research team of the Biotransport and Biomechanics laboratory here at National institute of technology, Rourkela for giving me an unforgettable experience during my postgraduate studies. There are too many of them to fit this small area, but each and every one of them is remembered for contributing, in one way or another, to the success of this work. I would like to specially thank to my fellow research workers and friends Krishna Reddy, Nakul Dewan and Protima a big thank you for without your humour, listening ears and assistance over a year I doubt this project would hold as special a place in my life. Thank you to my family who always support me no matter what course I embark, so you all become extra special supporters of this work. Lastly, I thank Almighty God with whose blessings I have reached at the completion of my research.

Date :
Place :

Rajeev Kumar Ranjan

Contents

Certificate of Approval i
Declaration iii
Curriculum Vita v
Acknowledgements vii
Contents ix
List of Figures xi
List of Tables xii
List of Symbols and Abbreviations xv
Abstract xvii

1 Introduction **1**
1.1 Background 2
1.1.1 Historical overview of Amperometric biosensor 2
1.2 Literature Review 4
1.3 Amperometric biosensor 5
1.3.1 Performance Factors or Biosensor characteristics 7
1.4 Damkohler Number 8

2 MATHEMATICAL MODELING **11**
2.1 finite volume method 12
2.2 Kinematic equations 13
2.2.1 Enzyme 13
2.2.2 Methods of Immobilization 14
2.2.3 Fick's second law 15
2.3 Model description 16
2.4 Initial and Boundary conditions 18

3 Results and discussion **21**
3.1 Contours of product concentration inside selective membrane 21
3.2 Variation of product concentration gradient along the axis 23
3.3 The effect of cylindrical and tapered perforation on current density 26
3.4 Conclusion 29

Bibliography **30**

List of Figures

1.1 Schematic diagram showing the main components of a biosensor The bio-reaction (a) converts the substrate to product. This reaction is determined by the transducer (b) which converts it to an electrical signal. The output from the transducer is amplified (c), processed (d) and displayed (e). . . . 1
1.2 Schematic diagram of an Amperometric biosensor 6
1.3 Block diagram of a biosensors 6

2.1 Enzyme-substrate interactions. 13
2.2 Structure of a biosensor with a perforated membrane 16
2.3 The profile of the unit cell 17

3.1 Product concentration for $r_2 = 0.1\mu m$ 22
3.2 Product concentration for $r_2 = 0.3\mu m$ 24
3.3 Product concentration for $r_2 = 0.5\mu m$ 25
3.4 Product concentration gradient along axis 27
3.5 Current density for tapered hole and cylindrical hole. 28

List of Tables

1.1 History of development of biosensors 3
1.2 Types of transducers required for the selective element [1] 7

3.1 Different values of enzyme volume and current density for different $r_2$values 28

LIST OF SYMBOLS AND ABBREVIATIONS

a	interfacial area (m^2)
C	cofactor concentration(μM)
C_0	initial concentration (μM)
$C^{'}$	cofactor product
$1-D$	one dimensional
$2-D$	two dimensional
d	enzyme membrane thickness (μm)
D_p	diffusion coefficient of product ($\mu m^2/s$)
D_s	diffusion coefficient of substrate ($\mu m^2/s$)
E	enzyme concentration (mM)
ES	complex of enzyme and substrate
f	any function
F	Faraday constant($9.64853 \times 10^4 C/moles\,of\,electrons$)
I	current density ($A/cm^2 \times 10^{10}$)
$ISFT$	ion-selective field effect transistor
K	rate constant
K_g	total mass transport coefficient
K_m	Michaelis-Menten constant(μM)
M	convective part
n_e	number of free electrons
P	product concentration (μM)
Q	source term
(r,θ,z)	cylindrical co-ordinate
$(r,\theta\varphi)$	spherical co-ordinate
S	substrate concentration (μM)
SAM	self assembled monolayer
SPR	surface plasma-resonance
k	thermal conductivity (W/mK)
M	convective part
t	time (s)
T	total time of residence (s)
V_{max}	maximum enzyme rate ($\mu M/s$)
$V(s)$	enzymatic reation rate ($\mu M/s$)
X	represents space
(x,y,z)	cartesian co-ordinates
Y	degree of conversion

Dimensionless Numbers

D_a	Damkohler number
$D_{a_{11}}$	other Damkohler number

Greek Letters

Ω	open region
$\overline{\Omega}$	closed region
$\triangle$	laplace operator
ν	outward normal vector
Ω_1	selective membrane region
Ω_2	enzyme layer region
ψ	third cylinder co-ordinate

ABSTRACT

The scope of this chapter is the advancements made in the area of amperometric biosensors. The main important discussion aspect is optimizing the biosensor's response. This paper deals with mathematical model for amperomatric Biosensor's outer perforated membrane in two dimensional (2-D) spaces. This model is based on reaction-diffusion mechanism. Model is consists of two layers, enzyme layer and selective layer. Our aim is to increase the accuracy of the biosensor response simulated by using 2-D model. To solve numerically, finite volume method is to be used. The biosensor response and the current density are investigated by changing the model parameter. We are using the Michaelis–Menten kinetics of an enzymatic reaction, which are nonlinear in nature. A novel approach of mathematical model is very useful in the detail study of substrate conversion. Mathematical modeling is nothing but a virtual experiments which is cost efficient through which immense kind of scientific analysis and prediction is possible. Relative influence of model parameters is dictated by a non-dimensional number called Damkohler number, which stated as 'the rate of enzymatic reaction to the rate of diffusion'. Our main focus is to analyse current density aftereffect of Damkholer number. Prior to our knowledge the current density of amperometric biosensors varies proportional in accordance with the concentration gradient of the reaction product at the electrode surface. And the current density of amperometric biosensors is proportional to the concentration gradient of the reaction product at the electrode surface.

Keywords: Biosensor, enzyme, amperometric, Damkholer number, perforated membrane, current density, diffusion.

CHAPTER 1

Introduction

Biosensor is an integrated device, capable of providing analytical information which consists of two components, a biological element usually an enzyme which detects the biological element, a transducer i.e. an electrode which converts the biological event into an electrical signal [2, 3] and present it to the end user. An amperometric biosensor measures the current that arises on the electrode due to the electrochemical reaction that occurs between the substrate and the biological element. The electrode is surrounded by a layer consisting of a biological element. The resultant current depends on the substrate concentration. Biosensors found a wide application in present day life due to its compatible characteristic features. Biosensors are highly sensitive and cheap devices. Biosensors are used in clinical diagnostics, environment monitoring, drug detection and food analysis. The schematic diagram of a biosensor is shown in the figure below:

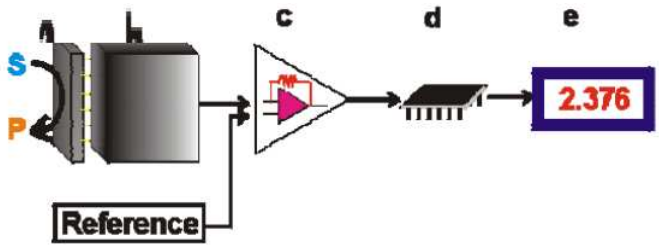

Figure 1.1: Schematic diagram showing the main components of a biosensor The bioreaction (a) converts the substrate to product. This reaction is determined by the transducer (b) which converts it to an electrical signal. The output from the transducer is amplified (c), processed (d) and displayed (e).

1.1 Background

For thirty years the analyte and electrode reactions has been an attractive approach for the development of biosensors. In 1962 the use of enzyme electrode was reported for the first time. The term biosensor is coined by Cammann in 1977. The architecture of a biosensor consists of bio-recognition element and a transducer, the bio-recognition element acts as the key feature of the biosensor, whose employment characterizes the performance of a biosensor. A variety of bio recognition element ranging from enzyme to antibodies is available for use. This information conveys the fundamental of biosensor for the development and optimization of a biosensor. The selection of the transducer material and transduction process depends on this information and the chemical approach for constructing the sensing layer around the transducer. In order to design a novel biosensor the choice of a bio-recognition element is very important. For a specific biosensor, the chosen redox enzyme must be suitable to selectively react with the analyte of interest. The selected enzyme is required to be stable under the operation as well as the storage conditions of then biosensor. The redox must be capable of providing reasonable long-term stability. One of the advantage of using the enzyme as the bio-recognition element is that they are easily available and are relatively cheap. In addition to this, the properties of the redox enzyme can be tuned accordingly by applying the required potential.

1.1.1 Historical overview of Amperometric biosensor

The first description of a biosensor was given for an Amperometric enzyme electrode for glucose in 1962 by Professor Leland C Clark, who is commonly known as the “Father of Biosensor”. In 1984 the Amperometric biosensor is further developed by introducing a mediator, referred as mediated Amperometric biosensor which utilizes ferrocene with glucose oxidase for glucose detection. Following the pioneering work by Kulys and Svirmickas were the first to show that an artificial redox mediator, ferrocene, could be employed for an amperometric glucose biosensor. As free – diffusing mediators, a large variety of compounds such as ferrocene derivatives, organic dyes, ferricyanide, ruthenium complexes and osmium complexes have been used [4]. Further research on biosensor provides self - monitoring devices for monitoring blood glucose levels which are successfully used by diabetes patients at home[5]. A different approach to realize biosensor architectures is the immobilization of a redox enzyme on the electrode surface in such a manner that direct electron transfer is possible between the active side of the enzyme and the transducer [6]. Thus, free - diffusing redox mediators are not necessary for these types of biosensors [7]. Biosensor designs based on direct electron transfer have been investigated thoroughly and comprehensively reviewed [6]. Therefore, a milestone was achieved when reversible electron transfer of cytochrome c was achieved for the first

Table 1.1: History of development of biosensors

Year	History of Biosensor Development
1916	First report on the immobilization of proteins: adsorption of invertase on activated charcoal
1922	First glass pH electrode
1956	Invention of the oxygen electrode (Clark)
1962	first description of a biosensor: an amperometric enzyme electrode for glucose (Clark)
1969	First potentiometric biosensor: urease immobilized on an ammonia electrode to detect urea
1970	Invention of the Ion-selective Field-Effect Transistor (ISFET) (Bergveld)
1972	First commercial biosensor: yellow springs Instruments glucose biosensor
1975	First microbe-based biosensor first immunosensor: ovalbumin on a platinum wire invention of the pO2 / pCO2
1976	First bedside artificial pancreas (Miles)
1980	First fibre optic pH sensor for in vivo blood gases
1982	First fibre optic-based biosensor for glucose
1983	First surface plasmon resonance (SPR) immunosensor
1984	First mediated amperometric biosensor: ferrocene used with glucose oxidase for the detection of glucose
1987	Launch of the MediSense ExacTechTM blood glucose biosensor
1990	Launch of the Pharmacia BIACore SPR-based biosensor system
1992	I-STAT launches hand-held blood analyser
1996	Glucocard launched
1996	Abbott acquires MediSense for $867 million
1998	Launch of LifeScan FastTake blood glucose biosensor
1998	Merger of Roche and Boehringer Mannheim to form Roche diagnostics
2001	LifeScan purchase Inverness Medical's glucose testing business for $1.3 billion
2003	i-STAT acquired by Abbott for $392 million
2004	Abbott acquires Therasense for $1.2 billion

time by employing tin - doped indium oxide electrodes [8] and 4,4´ - bipyridiyl as a promoting monolayer on gold electrodes [9, 10]. Starting from the 1980s self - assembled monolayers (SAM s) have received considerable attention in the scientific community and have been successfully employed in biosensors [11]. An example of bringing the electrode surface closer to the enzyme could be the introduction of conducting nanoparticles or nanostructures into the sensing layer in order to increase the probability of electron transfer taking place [12]. However, electron transfer efficiency is not only dependent on the distance of the involved redox relays but also on the properties of the electrode material, the nature of the enzyme, the properties of the immobilization matrix, and the redox mediator (if any) in a complex manner.

1.2 Literature Review

The mathematical model of an amperometric biosensor for investigating the dynamics of response of an amperometric biosensor with cyclic substrate conversion is presented by Baronas, Kulys, Ivanauskas [13].This model describes the substrate conversion taking place over a single enzyme membrane. The model is described using non-stationary diffusion equations containing non-linear term related to Michaelis–Menten kinetic of the enzymatic reaction. Finite difference technique is used for simulating the mathematical model. They have studied the effect of maximal enzymatic rate, substrate concentration and membrane thickness. From Baronas, Kulys, Ivanauskas [13] we know that the biosensor gain relatively increases with cyclic conversion at low substrate concentrations when the biosensor response is under diffusion control. In order to design an efficient biosensor, we consider an optimized model of a real biosensor. Schulmeister and Pfeiffer have represented the geometry of membrane perforation considering effective diffusion coefficient. They proposed 1-D in space mathematical model [14], they conclude that the quantitative value is limited. Later the biosensor with perforated membrane is developed into a 2-D mathematical model which is represented by Baronas et.al. [15, 16]. The 2-D model is used for investigating the numerical peculiarities for wide range of catalytic and geometrical parameters. However when the 2-D model is compared with 1-D model, 1-D simulation is found to be less time consuming. The comparison is more pronounced when Baronas and Petrauskas described a condition on which 1-D model can be applied directly to simulate the biosensor response accurately [17]. The accuracy of 1-D biosensor model is evaluated with that of the 2-D model. The 1-D in space mathematical model is suitable for simulating moderate operation of the biosensor. In turn the 2-D model is used for calculating the effective diffusion coefficient for usage in 1-D simulation.1-D model signifies inaccuracy when the holes of the perforated membrane are relatively very small, in such condition 2-D model is found to provide a better accuracy. Further analysis of amperometric biosensor considers similar approach previously discussed [15] , where the amperometric biosensor is modeled with selective membrane and perforated membrane. The response of an amperometric biosensor is simulated at mixed enzyme kinetics and diffusion limitation [18] varying the enzyme activity and substrate concentration. The resultant calibration graphs are different for transition state and steady state due to multi-concentration generation at the steady state condition. For a stable biosensor response it is important to select an appropriate membrane thickness [19]. It has been found that the maximal current increases with increase in membrane thickness when the enzyme kinetics predominate the biosensor response. The behavior of the biosensor response is also determined by the ratio of the enzyme-substrate reaction rate to the diffusion rate, providing the current is a function of the dimensionless thickness of the external diffusion layer [20].

1.3 Amperometric biosensor

After the volume of the literature regarding amperometric biosensors, we selected to the best of our knowledge and representative work that can be of use not only for the beginners but also for advance researches. A term 'amperometric biosensors' functioned by the production of a current when a potential is applied between two electrodes [2, 17]. Amperometric transducer allows for the electrometrical reactions to proceed at the electrode surface, giving rise to a current. The development of modern day amperometric biosensor has undergone three generations: The first generation amperometric biosensor involves the chemical reaction where the normal product of the reaction diffuses to the transducer and causes electrical response. The second generation amperometric biosensor deals with the improvement of the electrical response by employing an additional mediator (artificial mediator leads into a better biosensor response). And the third generation amperometric biosensor neither deals with the product nor with the mediator but the reaction does itself cause the response. An amperometric biosensor was developed by Updike and Hick's and reported the first practical amperometric biosensor using an enzyme electrode. Based on the types of analyte detection, the Amperometric biosensor can be modelled specifically like amperometric cholesterol biosensor, sandwich-type amperometric biosensor, PH sensitive amperometric biosensor, lactate amperometric etc. The simplest amperometric biosensors in common usage involve the Clark oxygen electrode. This consists of a platinum cathode at which oxygen is reduced and a silver/silver chloride reference electrode. When a potential of -0.6 V, relative to the Ag/AgCl electrode is applied to the platinum cathode, a current proportional to the oxygen concentration is produced. Normally both electrodes are bathed in a solution of saturated potassium chloride and separated from the bulk solution by an oxygen-permeable plastic membrane (e.g. Teflon, polytetrafluoroethylene). Amperometric biosensors are used in blood-diagnosis of diabetes, O_2 detection, H_2O_2 detection and Enzyme mediation. The schematic diagram of an Amperometric biosensor is given in figure 1.2:

$$S + C \overset{enzyme}{\longrightarrow} P + C'$$

Where; S = Substrate;
C = Cofactor / Coreactant;
P = Product;
C' = Cofactor Product

Amperometric biosensors exhibit some major drawback; it has shorter linear range and instability of the bio-molecules that can be partially solved by an application of an additional perforated membrane [17]. Schulmeister & Pfeiffer have already performed

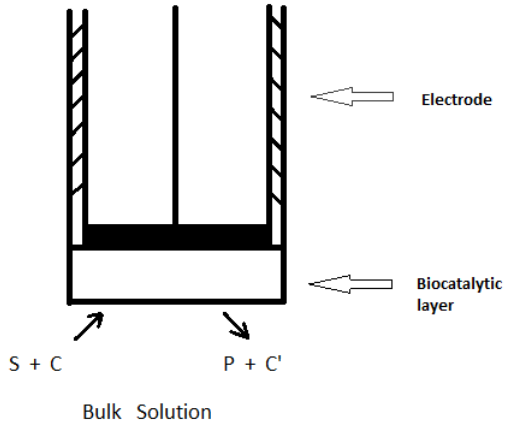

Figure 1.2: Schematic diagram of an Amperometric biosensor

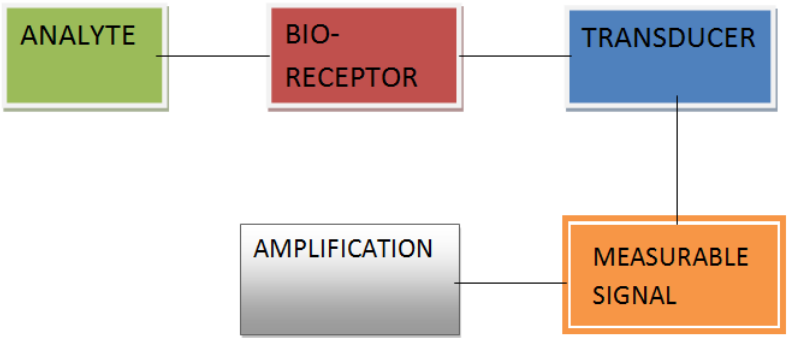

Figure 1.3: Block diagram of a biosensors

the Modelling of a biosensor configuration with a perforated membrane [2, 15]. The proposed one-dimensional in-space (1-D) mathematical model does not take into consideration the geometry of the membrane perforation. Theirs 1-D model have recognized that “its quantitative value is limited” [14][17]. In this paper, we investigate the conditions at which the 2-D mathematical model can be applied to simulate accurately the biosensor action. Enzymes show their poor stability in solutions, so we must need to stabilize the enzymes into the solution. There are various techniques available to stabilize the enzymes such as covalent linkage, physical adsorption, cross-linking, encapsulation and entrapment [21].

Above figure1.3 represents the block diagram of typical biosensors. Bio-receptor is a bio-molecule, which can identify the analyte target that has to be found out, but transducer is a component, which transforms the identified value into a particular signal that can be measured. These two components are integrated into a system to form a biosensor [19]. Biosensor is an analytical tool, which is combination of biochemical recognition component with a physical transducer [22]. The biochemical component serves to selectively catalyze a reaction or facilitate a binding event, and that biochemical recognition event allows the operation of biosensors in a complex sample matrix i.e. body

Table 1.2: Types of transducers required for the selective element [1]

SELECTIVE ELEMENT	TRANSDUCER
Synthetic Ionophores	Electrochemical –(current, potential, resistance, impedance)
synthetic carriers	-potentiometric
Supermolecular structures, cluster	-amperometric
Solid layers: metals	-conductimetric
- Metal oxides	-voltametric, poarographic
- Polymers, conducting polymers	-impedimetric, capacitive
Organisms	-piezoelectric
Micro-organisoms	Optical (florescence, light,scattering)
Plant & animal tissues	-transmission/absorbance/reflection
Cells	-dispersion, interferometric
Organelles	-polarimetric
Membranes, bilayers & monolayers	-circular dichroism, ellipsometry
Enzymes	-scattering
Receptors	-emission intensity, photon counting
Nucleic acids	Calorimetric (thermal, temperature)
Natural organic and inorganic molecules	Acoustic/ gravimetric (mass sensitive)

fluid. The most commonly electrochemical transducers used are based on amperometric and potentiometric. Type of transducers used classifies the biosensors like calorimetric, piezoelectric, optical and electrochemical biosensors [21].

1.3.1 Performance Factors or Biosensor characteristics

•**Selectivity**:- Selectivity is the ability of the sensor to respond only to the target analyte. That is, lack of response to other interfering chemicals is the desired feature.

•**Sensitivity range**:- Sensitivity is the response of the sensor to changes in analyte concentration.

•**Accuracy**:- This needs to be better than ±5%.

•**Nature of solution**:- Conditions such as pH, temperature and ionic strength must be considered.

•**Response time**:- This is usually much longer (30 s or more) with biosensors than with chemical sensors.

•**Recovery time**:- This is the time that elapses before the sensor is ready to analyse the next sample – it must not be more than a few minutes.

•**Life time** is the time period over which the sensor can be used without signif- icant deterioration in performance characteristics.

•**repeatablity**:- The output of the sensor has good repeatability if two sets of results obtained by the same operator, using the same sensor in the same sample, are close to each other.

•**reproduciblity**:- The system is reproducible if previous results can be obtained by workers in other laboratories. It is essential that a sensor has high reproducibility if it has to be used commercially.

•**Reversibility**:- The reversibility is the aptitude of the sensing mechanism to follow the variation of the environment.

•**range**:- Range is the concentration range over which the sensitivity of the sensor is good. Sometimes this is called dynamic range or linearity.

•**Detection limit** is the lowest concentration of the analyte to which there is a measurable response.

•**Stability** characterises the change in its baseline or sensitivity over a fixed period of time.

1.4 Damkohler Number

Damkohler Number is a dimensionless number. Basically it is used in a chemical analysis to relate time scale of chemical reaction to different phenomena which occurs in a system [23]. Damkohler number's definition changes according to the consideration of the system. So, many of Damkohler number may be possible [24].

Assuming any chemical reaction $A \rightarrow B$ of the order n

$$D_a = KC_0^{n-1} t \tag{1.1}$$

Where; K = rate constant of kinetics reaction

C_0 = Initial concentration

n = reaction order

t = time

It helps to estimate the degree of conversion (Y) in continuous flow reactor

Generally;

If $D_a < 0.1$ then $Y < 0.1$ and

If $D_a > 10$ then $Y > 0.9$

$$D_a = \frac{rate\,of\,reaction}{rate\,of\,convective\,mass\,transport} \quad or, \quad D_a = \frac{local\,fluid\,time}{local\,chemical\,reaction\,time} \tag{1.2}$$

In any type of reactor (continuous),

$$D_a = \frac{K_c C_0^n}{\frac{C_0}{T}} = K C_0^{n-1} T \tag{1.3}$$

here; 'T' is time of residence

At the time of mass transport interphase in a prone reacting system , the other Damkohler number ($D_{a_{11}}$) is assigned as the fraction of the rate of chemical reaction to the rate of mass transfer.

$$(D_{a_{11}}) = \frac{K C_0^{n-1}}{K_g a} \tag{1.4}$$

Where; $'K_g'$ is total mass transport coefficient and, 'a' is interfaced area.

CHAPTER 2

MATHEMATICAL MODELING

Mathematical modelling is a technique which builds on a firm understanding of the basic terminology, notation, and methodology of mathematics. It involves the following steps. First, the problem or objective of the study must be stated in a way that reflects accurately the needs of the organisation. The second step includes finding data relevant to the problem which can be applied to the model, and often includes the scaling of these measurements. This process often yields a more realistic model, the results of which are more easily comprehended. The third step in the modelling process is the development of a mathematical model that addresses the concerns of the organisation. In developing the mathematical model, the primary goal is to provide a quantitative structure for analysing a large group of possible situations. Model formulation frequently includes the selection of the appropriate mathematical functions to explain the phenomenon. In the fourth step, the data collected at the second step are applied to the mathematical model to obtain quantitative results. Step five involves the interpretation of the analysis completed in the previous step [25].

After a mathematical model of a continuous physical system, which may consist of, say, a set of differential equations and associated initial and boundary conditions, has been created, we try to obtain the solutions for this model. There are two kinds of solutions: exact analytical solutions and approximate solutions. Exact solutions can be obtained if we can solve an equation analytically, for example be able to solve a linear equation exactly. Approximate solutions can be obtained by applying some type of approximation to an equation or a system of equations.

In order to obtain an approximate solution, sometimes, the first thing we want to do is to non-dimensionalise the system. after the process of non-dimensionalisation, we end up with an equation or equations with dimensionless variables, rather than equa-

tions with a large number of physical parameters and variables all with dimensional units. The art of non-dimensionalisation lies in the choice of scales.

2.1 finite volume method

The finite-volume method is a discretization method that is especially advantageous for numerical investigations of partial differential equations in divergence form

$$\partial_t S(u) + \nabla.(M(u) - K(\nabla_u)) = Q(u) \tag{2.1}$$

where, 'S' is a storage term, 'M' is a convective part, 'K' is a diffusive part, and 'Q' is a source term. S, M, K, and Q can depend linearly or nonlinearly on u. It is also useful for partial differential equations where parts are in divergence form, for instance parabolic partial differential equations.

partial differential equations of first order

$$\nabla.q(u) = 0, \tag{2.2}$$

with nonlinear partial differential equations of higher order, systems of partial differential equations can be solved numerically with the finite- volume method.

we are consider the equation

$$\nabla.q(u) = f. \tag{2.3}$$

The first step of the finite-volume method is to partition the simulation domain Ω. The sub-domains Ω_i have to fulfill the following properties:

- each $\Omega_i$is open, simply connected, and has a polygonal border,
- $\Omega_i \cap \Omega_j = \emptyset \; for \; (i \neq j)$,
- $\bigcup_{i=1}^{M} \overline{\Omega}_i = \overline{\Omega}$.

The sub-domains are called control volumes or control areas. The next step is to integrate (3) over the control volume Ωi and use the divergence theorem yielding

$$\int_{\partial\Omega_i} \nu.q(u)\, d\sigma = \int_{\Omega_i} f\, dx, \;\; i \epsilon \{1, ..., M\} \tag{2.4}$$

where ν is the outward pointing normal vector on $\partial\Omega_i$. Because of our requirements, the border $\partial\Omega_i$ consists of n_i lines. So we can write (4) as

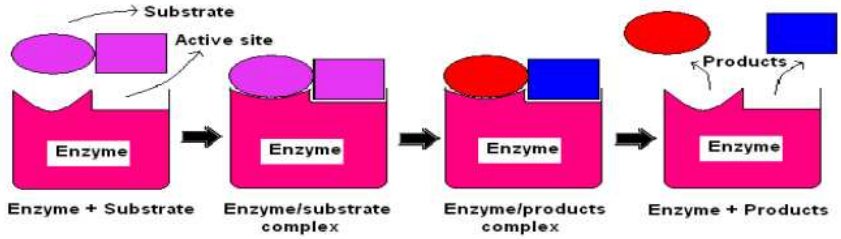

Figure 2.1: Enzyme-substrate interactions.

$$\sum_{j=1}^{n_i} \int_{\Gamma_{ij}} \nu_{ij}.q(u)d\sigma = \int_{\Omega_i} f\,dx \tag{2.5}$$

The last step is to discretize the integrals in (5).

2.2 Kinematic equations

2.2.1 Enzyme

An enzyme (figure2.1) has a specific three-dimensional shape, it is a large molecule, usually much bigger than its corresponding binding substrate. Only a relatively small part of the enzyme called its active site actually comes into contact with the substrate. Part of the substrate fits into the active site and forms a temporary structure called an enzyme-substrate complex. The substrate molecule is like the key that fits the enzyme's lock. The reaction takes place at the active site and this is where the products are formed. As the products have a different shape from the substrate, they no longer fit the active site and are repelled. The active site is then free to react with more substrates. The active site of the enzyme may not exactly correspond to the shape of the substrate, as the active site has a more flexible shape and therefore it is able to mould itself around the substrate.

An enzyme biosensor figure consists of an enzyme as a biological sensing element and a transducer, which may be amperometric, potentiometric, conductimetric, optical, calorimetric, etc. Enzyme biosensors have been applied to detecting various substrates, which are selectively oxidised or reduced in enzyme-catalysed processes depending on the nature of the substrates and enzymes used (oxidases or reductases) to construct a sensor. Most enzyme biosensors modelled in this thesis use amperometric techniques [26]. Amperometry is the determination of the intensity of the current crossing an electrochemical cell under an imposed potential. This intensity is a function of the concentration of the electrochemically active species in the sample. Oxidation or reduction of a species is generally performed by a working electrode, and a second electrode acts as a reference. For example, a glucose-sensitive biosensor that uses glu-

cose oxidase could detect either the H_2O_2 produced by the enzymatic reac- tion, or the amount of oxygen consumed during the oxidation of glucose [27].

2.2.2 Methods of Immobilization

The selective element must be connected to the transducer. This presents partic- ular problems if the former is biological in nature. Several classes of methods of connection have evolved, as follows:

• The simplest method is adsorption on to a surface.

• Microencapsulation is the term used for trapping between membranes – one of the earliest methods to be employed.

• Entrapment, where the selective element is trapped in a matrix of a gel, paste or polymer – this is a very popular method.

• Covalent attachment, where covalent chemical bonds are formed between the selective component and the transducer.

• Cross-linking, where a bifunctional agent is used to bond chemically the transducer to the selective component – this is often used in conjunction with other methods, such as adsorption or microencapsulation.

The amperometric biosensor is treated as an electrode and enzyme is comparably thin layer, which further applied onto the surface of electrode. This model includes enzyme layer where the enzymatic reaction occurs as well as the mass transfer by diffusion takes place. In enzyme layer analyte concentration is maintained constant [17]. At the time during an enzyme catalyzed reaction,

$$E + S \longleftrightarrow ES + P$$

where;

S= substrate;

E= enzyme;

ES= complex;

P= product

Product formation rate mainly rely upon the substrate concentration [17, 28]. At steady state condition, we neglect the diffusion of substrate and product molecules, and with the help of Michaelis-Menten equation we can have the mathematical model of enzyme kinetics is

$$V(s) = \frac{dp}{dt} = -\frac{ds}{dt} = \frac{V_{max}.S}{K_m + S} \tag{2.6}$$

where, V(s) is the enzymatic reaction rate, V_{max} is the maximum enzymatic rate achievable with that quantity of enzyme, when substrate is fully saturated by enzyme, K_m is Michaelis constant; S is the concentration of substrate; P is the concentration of product and 't' is the time [29, 30]. At the electrode surface the reaction product is implied into an electrochemical reaction where some free electrons are discharged. That discharged electrons causes the electrical signal which is further amplified. In the case of amperometry the biosensor current is in proportion with the concentration of the substrate (target analyte) [17].

A proposed biosensor contains a multilayer enzyme membrane. Electrode is covered by the selective membrane which acts as transducers. The detection limit of the enzyme electrodes depends on the sensitivity of the amperometric system [31].

The enzyme-catalyzed reaction is described by Fick's second law, the system of equations are- [30, 32].

$$\frac{\partial S}{\partial t} = D_s \frac{\partial^2 S}{\partial x^2} - \frac{V_{max}.S}{K_m + S'}$$

$$\frac{\partial P}{\partial t} = D_p \frac{\partial^2 P}{\partial x^2} + \frac{V_{max}.S}{K_m + S'} \quad 0 < x < d;\ t > 0 \tag{2.7}$$

Where S(x, t) and P(x, t) are the concentration of substrate and product respectively, t represents time and x for space. D_p and D_s represents the diffusion coefficient of the product and substrate respectively. K_m is Michaelis-Menten constant when the enzyme is fully saturated with substrate, V_{max} is the maximal enzymatic rate; d is enzyme membrane thickness [33].

2.2.3 Fick's second law

Fick's second law or diffusion equation is a combined result of Fick's first law and the equation of continuity. It is second order partial differential equation. [34, 35].

$$\frac{\partial C}{\partial t} = \nabla.(D \nabla C) \tag{2.8}$$

If 'D' depends on concentration then it is nonlinear in nature. And if the diffusivity is independent of concentration equation 2.8 simplifies to

$$\frac{\partial C}{\partial t} = D \triangle C \tag{2.9}$$

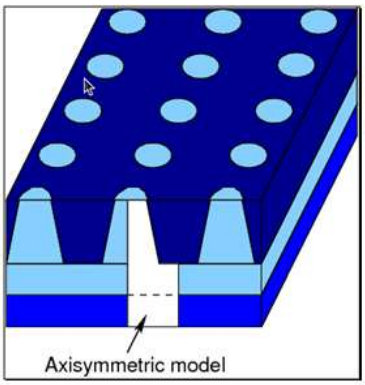

Figure 2.2: Structure of a biosensor with a perforated membrane

; Where Δ is Laplace operator

This form of Fick's second law also called the linear diffusion equation. It is a linear second order partial differential equation for the concentration field C (x, y, z, t). On the right hand side of equation 2.9, Δ has different representation in different coordinate systems. dg[35–37].

Cartesian coordinates (x, y, z):

$$\frac{\partial C}{\partial t} = D\left(\frac{\partial^2 C}{\partial x^2} + \frac{\partial^2 C}{\partial y^2} + \frac{\partial^2 C}{\partial z^2}\right) \tag{2.10}$$

Cylindrical coordinates (r, ϑ , z):

$$\frac{\partial C}{\partial t} = \frac{D}{r}\left[\frac{\partial}{\partial r}\left(r\frac{\partial C}{\partial r}\right) + \frac{\partial}{\partial \theta}\left(\frac{1}{r}\frac{\partial C}{\partial \theta}\right) + \frac{\partial}{\partial z}\left(r\frac{\partial C}{\partial z}\right)\right] \tag{2.11}$$

Spherical coordinates (r, ϑ, φ):

$$\frac{\partial C}{\partial t} = D\left[\frac{\partial^2 C}{\partial r^2} + \frac{2}{r}\frac{\partial C}{\nabla r} + \frac{1}{r^2 sin^2\theta}\frac{\partial^{2C}}{\partial \varphi^2} + \frac{1}{r^2}cot\theta\frac{\partial C}{\nabla \theta}\right] \tag{2.12}$$

2.3 Model description

The above figure 2.2 is axisymmetric model of biosensors. Each holes in the perforated membrane considered as a tapered cylinder having non-uniform diameter. Whole biosensor is divided into equal hexagonal prism having regular bases. We are considering area of circle is equal to the area of hexagon. One cylinder is considered as unit cell.

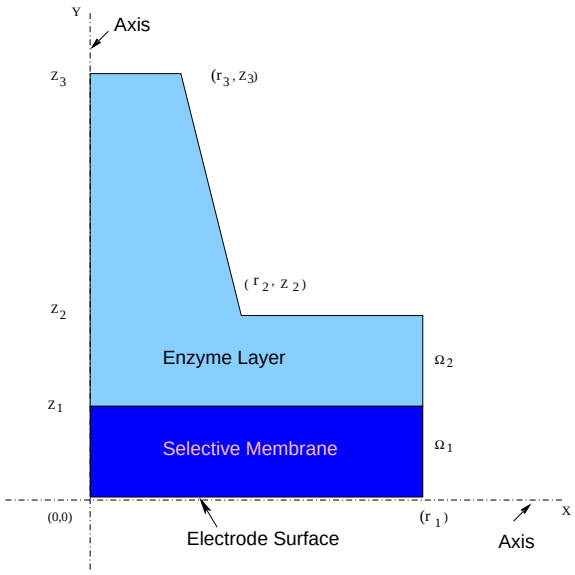

Figure 2.3: The profile of the unit cell

Above figure 2.3 shows profile of the unit cell of biosensors, where Ω_1 represents the selective membrane and Ω_2 represents the enzyme layer region. Assuming horizontal line as X-axis and vertical line as Y-axis.

Selective membrane (Ω_1):

[$0 \leq r \leq r_2$, $0 \leq z \leq z_1$]

Enzyme region (Ω_2):

[$0 \leq r \leq r_1$, $z_1 \leq z \leq z_2$] U [$0 \leq r \leq r_{slant}$, $z_2 \leq z \leq z_3$]

Equation of slant line,

$$\frac{r - r_3}{r_2 - r_3} = \frac{z - z_3}{z_2 - z_3}$$

$$r = r_3 + (\frac{r_2 - r_3}{z_3 - z_2}).(z - z_3) = r_{slant} \tag{2.13}$$

Where, r_1 is base of unit cell, r_2 and r_3 are the x-axis co-ordinates of outer perforated membrane, z_1 is the thickness of the selective membrane, $(z_2 - z_1)$ is the thickness of the enzyme layer and $(z_3 - z_2)$ is the thickness of perforated membrane. We are assuming that holes are fully filled with enzyme.

In selective membrane region (Ω_1), mass transfer is taking place due to diffusion of product,

$$\frac{\partial P_1}{\partial t} = D_1 \triangle P_1,\ (r, z)\, \epsilon\, \Omega_1,\ t > 0 \tag{2.14}$$

where,

$P_1$is product concentration in $\overline{\Omega}_1$.

D_1 diffusion coefficient of the product in the selective membrane.

$\triangle$ is the Laplace operator. There is no substrate in Ω_1.

In the region Ω_2, the enzymatic reaction and diffusion take place and concentration is described by reaction-diffusion equation ($t > 0$).

$$\frac{\partial S_2}{\partial t} = D_1 \triangle S_2 - R(S_2),$$

$$\frac{\partial P_2}{\partial t} = D_2 \triangle P_2 + R(S_2)\,,\ (r\,,\,z)\,\epsilon\,\Omega_2 \tag{2.15}$$

Where, S_2 and P_2 are the substrate and product concentration in $\overline{\Omega}_2$.

For simplicity, we assume that diffusion coefficient for both substrate and product are same .

As we know the current density of the amperometric biosensor is proportional to the concentration gradient of the reaction product at the electrode surface.

$$i(t) = n_e F D_1 \frac{1}{\pi r_2^2} \int_0^{2\pi} \int_0^{r_2} \frac{\partial P_1}{\partial z} |_{z=0}\ r\,dr\,d\psi$$

$$i(t) = n_e F D_1 \frac{2}{r_2^2} \int_0^{r_2} \frac{\partial P_1}{\partial z} |_{z=0}\ r\,dr \tag{2.16}$$

Where, $i(t)$= current density at time t,

ψ= third cylindrical coordinate

n_e=number of electrons emitted in the reaction

F= Faraday constant

The stationary current is-

$I = lim_{t\to\infty} i(t)$; Where, I is current density of steady state .

2.4 Initial and Boundary conditions

(A) Initial conditions (t=0) for substrate and products are...

(1) Initial condition for substrate:

S (r, z, 0) = 0, in enzyme region (i.e. $0 \le r \le r_1$, $z_1 \le z \le z_2$), at time t=0

S (r ,z, 0) = S_0, in the perforated membrane region (i.e. $0 \le r \le r_{slant}$, $z_2 \le z \le z_3$), at time t=0, and

S (r, z, 0) = 0, in the selective membrane region (i.e. $0 \le r \le r_2$, $0 \le z \le z_1$)

(2) initial condition for product

P_i(r, z, 0) = 0, $\in \overline{\Omega}_i$, where, i = 1,2.

(B) Boundary conditions for the profile unit cell.

$$\frac{\partial P_1}{\partial r}\,|_{r=0} = \frac{\partial P_1}{\partial r}\,|_{r=1} = 0,\ (0 \le z \le z_1) \tag{2.17}$$

It means initially at time, t=0 the product concentration gradient inside the selective membrane region is zero.

$$\frac{\partial S}{\partial r}\,|_{r=0} = \frac{\partial P_2}{\partial r}\,|_{r=0} = 0,\ (z_1 \le z \le z_3) \tag{2.18}$$

$$\frac{\partial S}{\partial r}\,|_{r=r_1} = \frac{\partial P_2}{\partial r}\,|_{r=r_1} = 0,\ (z_1 \le z \le z_2) \tag{2.19}$$

At the electrode surface, electrochemical reaction of the product occurs because the nature of the product is electro-active. At the electrode surface, to maintain the product concentration zero, we choose the electrode potential accordingly. i.e.

$$P_1(r, 0, t) = 0 \quad (0 \le r \le r_2) \tag{2.20}$$

Boundary conditions for the upper boundary of enzyme membrane region ($0 \le r \le r_3$). Where the concentration of substrate and product are constant for the total time of biosensor action.

$$S(r, z_3, t) = S_0,\ and\ \ P_2(r, z, t) = 0,\ \ for\ (0 \le r \le r_3). \tag{2.21}$$

We assume there is no leakage of flux at the boundary of perforated membrane. i.e.

$$\frac{\partial S}{\partial r}\,|_{r=r_{slant}} = \frac{\partial P_2}{\partial r}\,|_{r=r_{slant}} = 0 \tag{2.22}$$

$$\frac{\partial S}{\partial z}\,|_{z=z_2} = \frac{\partial P_2}{\partial z}\,|_{z=z_2} = 0,\ \ (r_2 \le r \le r_1) \tag{2.23}$$

CHAPTER 3

Results and discussion

The effect of perforated membrane geometry on the biosensor response is studied using numerical modeling. The biosensor response is quantified by the current density. The current density is obtained for the selective membrane thickness of 2μm, the enzyme layer thickness of 2μm, and the thickness of the perforated membrane of 10μm. The geometry of the biosensor is varied by varying the slantness of the regular cylindrical shape of the hole inside the perforated membrane. The top radius is kept fixed at $0.1\mu m$ while the bottom part is varied with a dimension of $0.1\mu m$, $0.3\mu m$, and $0.5\mu m$. The bottom part with a dimension of $0.1\mu m$ gives a regular cylindrical hole inside the perforated membrane. The current density thus obtained for a slant geometry is compared with that of the regular geometry.

3.1 Contours of product concentration inside selective membrane

Figure 3.1 shows the contours of product concentration inside the selective membrane for the time instances of t=2s, 4s, 6s, and 8s for a perforated membrane with a cylindrical hole having inner radius $0.1\mu m$. It can be noticed that with the increase in time from 2s to 4s there is an increase in the concentration of product inside the selective membrane from 0.002 μM to $0.0035\mu M$ at the top. This is quite obvious because with the increase in time, until the steady state is reached, the substrate keeps on depleting itself in the presence of enzyme and subsequently more amount of product is formed. Also, the contour of $0.0005\mu M$ product concentration shifts towards the electrode indicating an increase in the product gradient near the electrode surface. With the further increase in

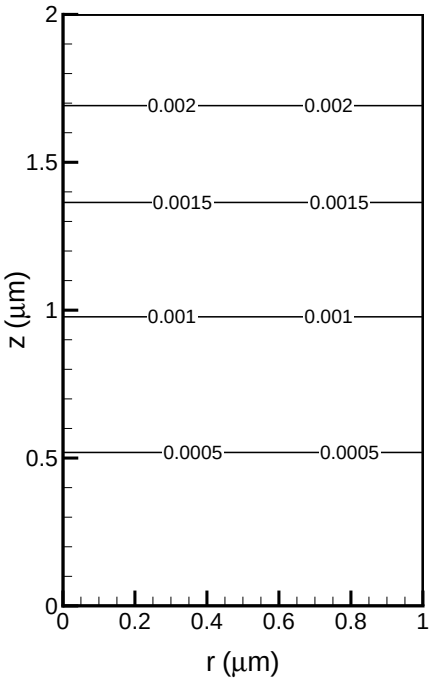

(a) at time = 2 s

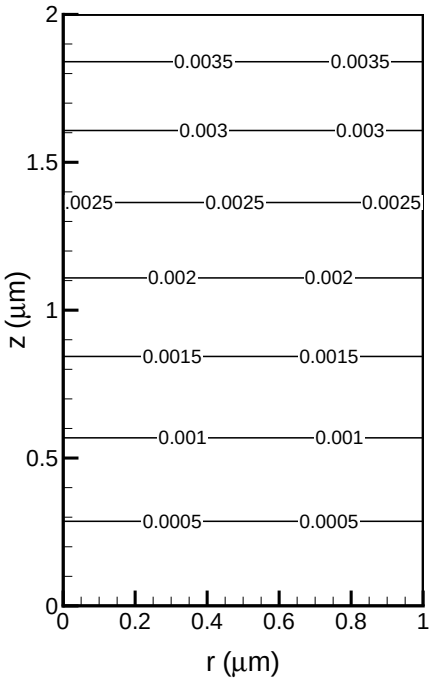

(b) at time = 4 s

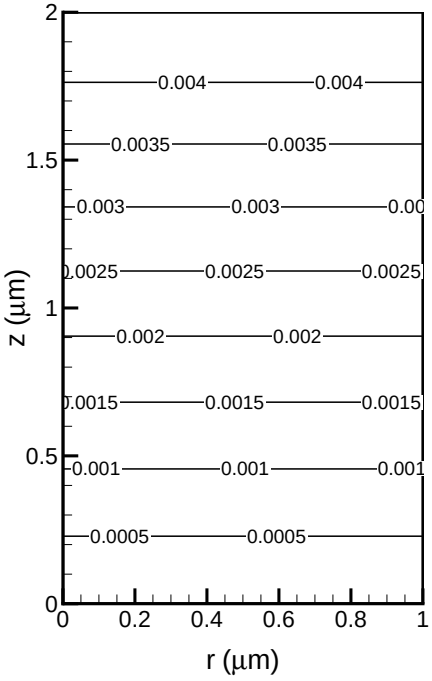

(c) at time = 6 s

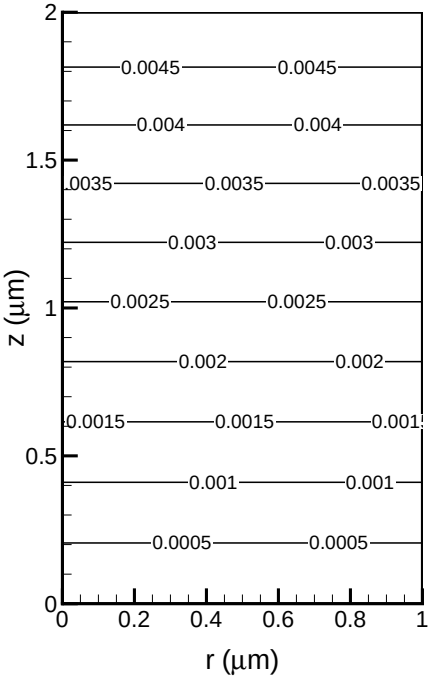

(d) at time = 8 s

Figure 3.1: Product concentration for $r_2 = 0.1\mu m$

time from 4s to 6s, it can be observed that the contour of $0.0005\mu M$ product concentration shifts more towards the electrode surface. Also, the maximum concentration inside the selective membrane increases from $0.0035\mu M$ to $0.004\mu M$. But, when the time increases to 8s the shiftment of contour of $0.0005\mu M$ product concentration towards the electrode surface is less indicating that the configuration is attaining its steady state.

Figure 3.2 shows the contours of product concentration inside the selective membrane for the time instances of t=2s, 4s, 6s, and 8s for a perforated membrane with a tapered hole having bottom radius = $0.3\mu m$ and top radius = $0.1\mu m$. It can be noticed that with the increase in time from 2s to 4s there is an increase in the concentration of product inside the selective membrane from 0.007 μM to $0.01\mu M$ at the top. This is quite obvious because with the increase in time, until the steady state is reached, the substrate keeps on depleting itself in the presence of enzyme and subsequently more amount of product is formed. The concentration of product is more for this case as compared to the previous case of a cylindrical hole. This can be attributed to the fact that a tapered hole would contain an increased amount of enzyme as compared to the corresponding case of a cylindrical hole. As a consequence, product formation is more. Also, the contour of $0.001\mu M$ product concentration shifts towards the electrode indicating an increase in the product gradient near the electrode surface. But, this increase is less as compared to the previous case. With the further increase in time from 4s to 6s, it can be observed that the contour of $0.001\mu m$ product concentration shifts more towards the electrode surface. Also, the maximum concentration inside the selective membrane increases from $0.01\mu M$ to $0.011\mu M$. But, when the time increases to 8s the shiftment of contour of $0.01\mu M$ product concentration towards the electrode surface is negligible indicating that the configuration has attained its steady state. It should be noted that with increase in the amount of enzyme, the steady state is reached earlier.

When the slantness of the tapered hole is increased more by selecting bottom radius = $0.5\mu m$ and top radius = $0.1\mu m$, the product concentration further increases from $0.007\mu M$ to $0.01\mu M$ at the top and $0.001\mu M$ to $0.002\mu M$ at the bottom at a time instant of 2s as shown in the figure 3.3. As observed for other cases, the concentration of product increases with increase in the time. But, for this case, the steady state is reached much earlier than the other two cases.

3.2 Variation of product concentration gradient along the axis

The product concentration gradient for both cylindrical and tapered hole with axial distance from the biosensing electrode is also analyzed since the product concentration gradient affect sensitivity of an amperometric biosensor. In this work, variations in

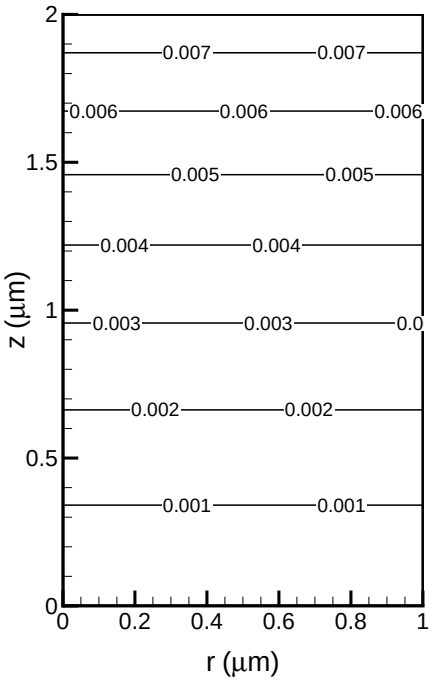

(a) at time = 2 s

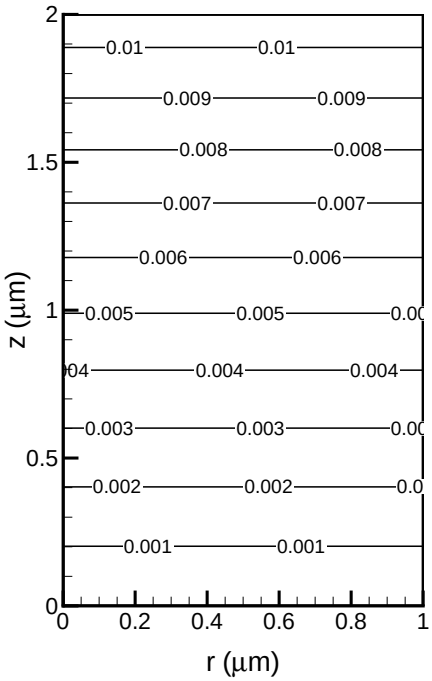

(b) at time = 4 s

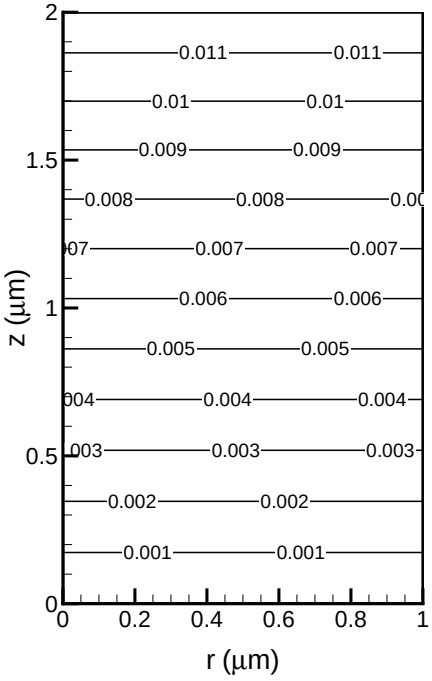

(c) at time = 6 s

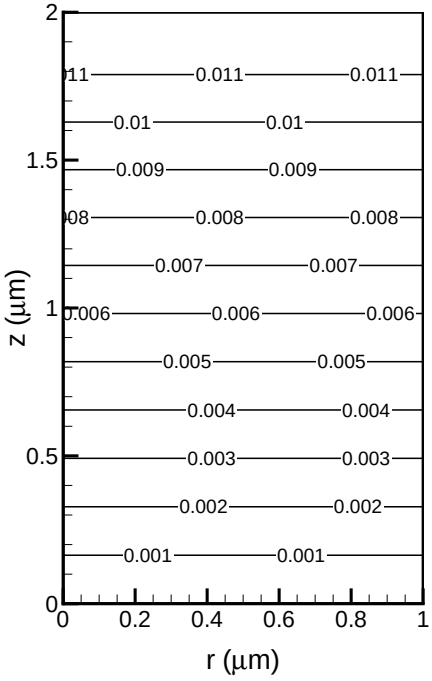

(d) at time = 8 s

Figure 3.2: Product concentration for $r_2 = 0.3\mu m$

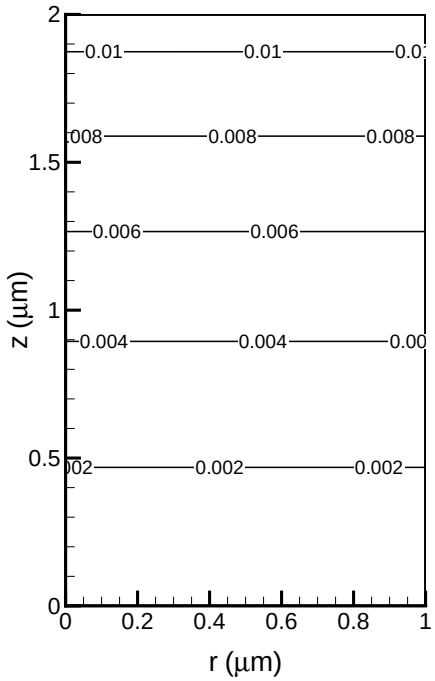

(a) at time = 2 s

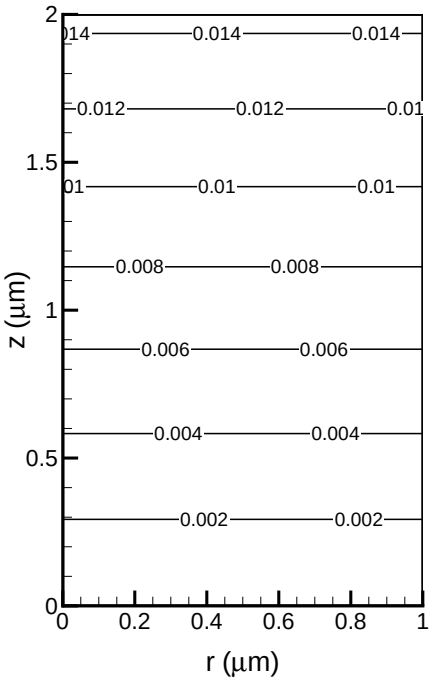

(b) at time = 4 s

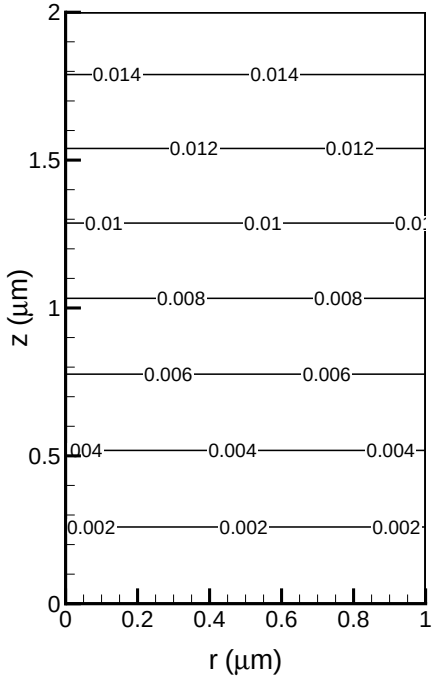

(c) at time = 6 s

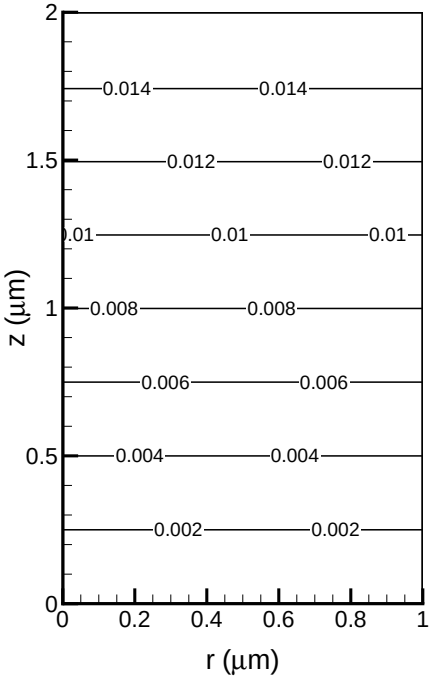

(d) at time = 8 s

Figure 3.3: Product concentration for $r_2 = 0.5\mu m$

product concentration gradient along the z-axis at different values of r_2 is analyzed with respect to time. The gradient of product concentration along the axis for the studied configurations is shown in figure 3.4. Figures 3.4a, 3.4b, and 3.4c show the gradient of product concentration for a cylindrical hole with a radius of $0.1\mu m$, a tapered hole with a bottom radius of $0.3\mu m$, and a tapered hole with a bottom radius of $0.5\mu m$ respectively. The gradient is plotted for the four time instances of 2s, 4s, 6s, and 8s during the enzymatic reaction. It can be noticed that there is discontinuity in the variation of product gradient. The gradient is discontinuous at z = $2\mu m$ and z = $4\mu m$ for the case of a cylindrical hole (see figure 3.4a). It should be noted that the region between z = $0\mu m$ and z = $2\mu m$ is the region of selective membrane, between z = $2\mu m$ and z = $4\mu m$ is the region of enzyme layer and rest is the region of tapered hole (perforated membrane). It can be seen that during the first 2s of the enzymatic reaction the product gradient in the perforated membrane has almost reached the steady state but, inside the selective membrane it is still in its transient state. But with the progress of time, even the product gradient inside the selective membrane reaches its steady state. The interesting observation which can be inferred from the figure is that throughout the reaction the product gradient is almost zero inside the enzymatic layer, i.e. the region between z = $2\mu m$ and z = $4\mu m$.

When the bottom radius of the hole is increased to $0.3\mu m$, the discontinuity at z = $4\mu m$ reduces. This can be attributed to the fact that with the increase in the bottom radius the sharpness at the junction of enzymatic layer and the perforated membrane layer decreases which smoothens out the discontinuity. This discontinuity further reduces when the bottom radius of the tapered hole is increased to $0.5\mu m$ (see figure 3.4c). But, similar trend is observed inside the region of selective membrane. Also, with the increase in the slantness of the hole, the steady state value of product gradient at the electrode surface, i.e. z = $0\mu m$, increases. Thus it can be concluded that the presence of tapered hole increases the product concentration gradient at the electrode surface as compared to the case of cylindrcal hole, which improves the sensitivity of biosensor.

3.3 The effect of cylindrical and tapered perforation on current density

The effect of the perforation level and geometry of the perforated hole is quite significant for the sensitivity of an amperometric biosensor. In order to investigate the effect of cylindrical perforation and tapered perforation over current density, the biosensor response is simulated with top radius fixed at $0.1\mu m$ while changing the bottom radius to $0.1\mu m$, $0.3\mu m$, and $0.5\mu m$. The result is presented in figure 3.5. It can be seen that with increase in the taperedness the time taken for current density to reach steady state

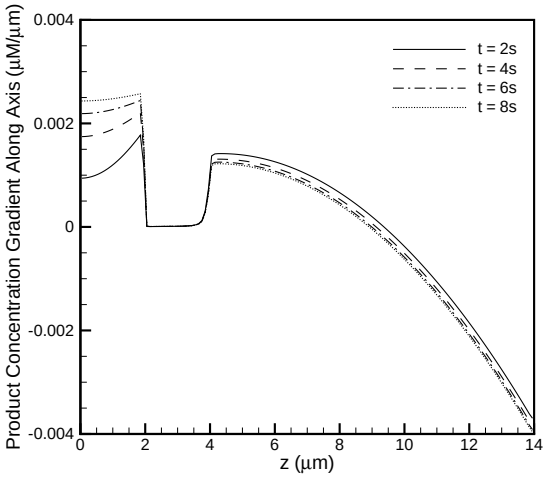

(a) at $r_2 = 0.1\mu m$

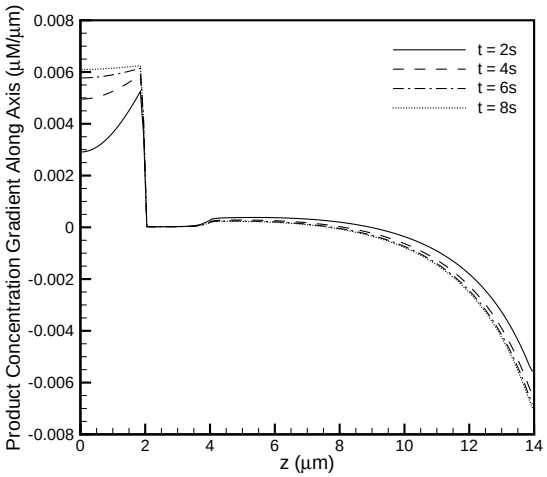

(b) at $r_2 = 0.3\mu m$

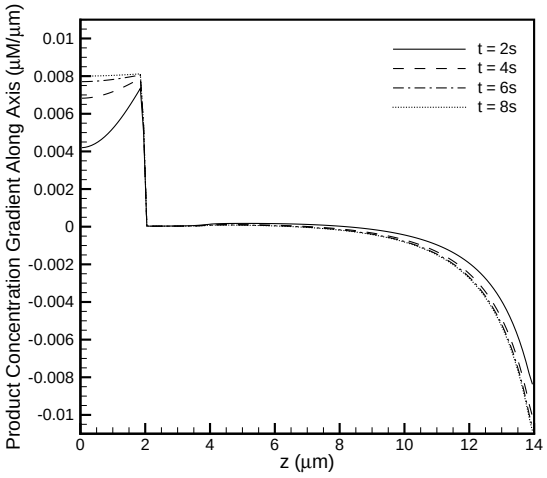

(c) at $r_2 = 0.5\mu m$

Figure 3.4: Product concentration gradient along axis

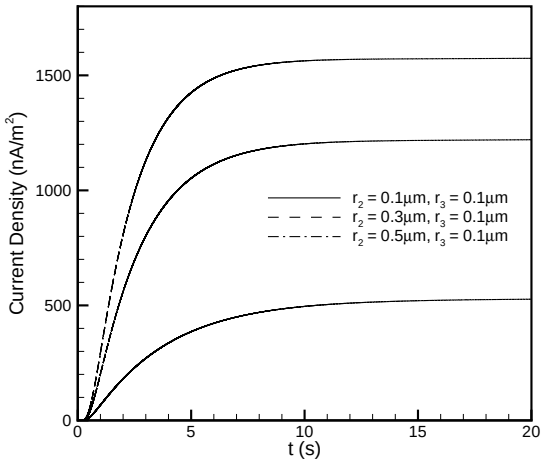

Figure 3.5: Current density for tapered hole and cylindrical hole.

Table 3.1: Different values of enzyme volume and current density for different $r_2$values

$r_3\,(\mu m)$	$r_2\,(\mu m)$	enzyme volume (μm^3)	% increase in volume	current density (I), nA/m^2	% increase in current density
0.1	0.1	6.597	—	526	—
0.1	0.3	7.644	15.87	1220.11	131.94
0.1	0.5	9.529	44.44	1573.98	199

decreases which is also observed in the previous section. Also, with increase in the taperedness the value of steady state current density also increases. The value of steady state current density for the studied case is listed in table 3.1. It can be seen that in the case of a cylindrical hole the output value of current density is 500 nA/m^2 and in the case of tapered hole when $r_2 = 0.3\mu m$ it is 1200 nA/m^2 and when$r_2 = 0.5\mu m$ it is 1573 nA/m^2. It means that the current density is approximately doubled when r_2 is changed from $0.1\mu m$ to $0.3\mu m$ and it is approximately trippled when r_2 is changed from $0.1\mu m$ to $0.5\mu m$. But, the interesting observation is that the biosensor response is tripped only for a marginal increase in the enzyme volume by 44%.

Thus, it can be concluded that changing the geometry of holes has great impact on the efficiency of biosensor. In this mathematical modeling, in order to get higher current density tapered cylindrical holes are considered. As the internal radius increases, the enzyme volume also increases gradually, which leads to an increase in the current density. But, this increase in the current density comes at an insignificant increase in the enzyme volume. Thus, it indicates that tapered perforated membrane leads to a higher sensitivity of an amperometric biosensor.

3.4 Conclusion

The response of an amperometric biosensor is studied using two dimensional numerical modeling. The effect of perforated membrane geometry on biosensor response is studied and It has been shown that changing the geometry of holes has great impact on the efficiency of biosensor. The current density is found to increase with the increase in the taperedness of the perforated membrane hole. The current density increases by three fold when the bottom radius of the preforated membrane hole is increased from $0.1\mu m$ to $0.5\mu m$. This increase is achieved by merely increasing the enzyme volume by 44%. Also, it has been observed that with increase in the taperedness the time taken for current density to reach its steady state value decreases.

Bibliography

[1] Spichiger-Keller U.E., Chemical sensors and Biosensors for Medical and Biological Applications., Wiley-VCH. .

[2] A. Turner, I. Karube, G. wilson, Biosensors: Fundamentals and Applications., Oxford university Press, Oxford., 1987.

[3] F. Scheller, F. schubert, Biosensors., Elseiver, Amsterdam. 7.

[4] P. Bartlett, P. Tebbutt, R. Whitaker, Kinetic aspects of the use of modified electrodes and mediators in bioelectrochemistry., progress in Reaction Kinetics. 16 ((2)) (1991) 55–155.

[5] J. Newman, A. Turner, Home blood glucose biosensors: a commercial perspective., Biosensors & Bioelectronics. 20 ((12)) (2005) 2435–2453.

[6] J. Frew, H. Hill, Review: direct and indirect electron transfer between electrodes and redox proteins., E uropean Journal of Biochemistry. (1988) 172, 261–269.

[7] J. Kulys, A. Samalius, G. Svirmickas, Electron exchange between the enzyme active and organic metals ., FEBS Letters. (1980) 114, 7–10.

[8] P. Yeh, T. Kuwana, Reversible electrode reaction of cytochrome., Chemistry Letters. 6 ((10)) (1977) 1145–1148.

[9] M. Eddowes, H. Hill, Novel method for the investigation of the electrochemistry of metalloproteins. cytochrome c ., Journal of the Chemical Society. Chemical Communications. (1977) 771–772.

[10] M. J. Eddowes, H. A. O. Hill, K. Uosaki, The electrochemistry of cytochrome c. Investigation of the mechanism of the 4,4' - bipyridyl surface modified gold electrode., Bioelectrochemistry and Bioenergetics. 7 (3) (1980) 527–537.

[11] R. Nuzzo, D. Allara, Adsorption of bifunctional organic disulfi des on gold surfaces., Journal of the American Chemical Society. 105 ((13)) (1983) 4481–4483.

[12] E. Katz, I. Willner, Integrated nanoparticle-biomolecule hybrid systems: synthesis, properties, and applications ., Angewandte Chemie International Edition. 43 ((45)) (2004) 6042–6108.

[13] Romas Baronas., Juozas Kulys., Feliksas Ivanauskas., Modelling amperometric enzyme electrode with substrate cyclic conversion. .

[14] T. Schulmeister, D. Pfeiffer, Mathematical modelling of amperometric enzyme electrodes with perforated membranes., Biosens. Bioelectron. 8 (1993) 75–79.

[15] R. Baronas, J. Kulys, F. Ivanauskas, Computational modelling of biosensors with perforated and selective membranes., J. Math. Chem. 39 ((2)) (2006) 345–362.

[16] R. Baronas, Numerical simulation of biochemical behaviour of biosensors with perforated membrane., in: Proc. 21st European Conference on Modelling and Simulation ECMS 2007, Zelinka, Z. Oplatkova, A. Orsoni (Eds.). (2007) 214–217.

[17] K. Petrauskas, R. Baronas, Computational Modelling of Biosensors with an Outer Perforated Membrane, Nonlinear Analysis., Modelling and Control, 14 ((1)) (2009) 85–102.

[18] J. Kulys, R. Baronas, Modeling of Amperometric biosensors in the case of substrate inhibition., Sensors. .

[19] R. Baronas, J. Kulys, F. Ivanauskas, The influence of the enzyme membrane thickness on thye response of Amperometric biosensors., Sensors . .

[20] J. Kulys, R. Baronas, Modeling Amperometric biosensor based on chemically modified electrodes., Sensors. .

[21] B. Malhotra, A. Chaubey, Sensors and Actuators. B 91 (2003) 117–121.

[22] Nikhil., k. Amitesh., numerical modelling of an amperometric biosensor., Tech. Rep. 8-20, NIT, Rourkela, 2012.

[23] T.-L. Jiang, E. E. O'Brien., Schmidt, Damkohler and Reynolds number effects on second-order reactions in isotropic turbulence., Chemical Engineering Communications. 106 ((1)) (1991) 185–206.

[24] S. Fogler, Elements of Chemical Reaction Engineering., NJ: Pearson Education, ISBN 0-13-047394-4., (4th ed.) edn., 2006.

[25] C. Lin, L. Segel, Mathematics Applied to Deterministic Problems in the Natural Sciences., Published by SIAM. .

[26] L. Gorton, Biosensors and Modern Biospecific Analytical Techniques., Published by Elsevier B.V. .

[27] T. Canh, Biosensors., Chapman & Hall and Masson., 1993.

[28] R. Baronas, F. Ivanauskas, J. Kulys, Computer Simulation of the Response of Amperometric biosensors in Stirred and non Stirred Solution., Nonlinear Analysis: Modelling and Control. 8 ((1)) (2003) 3–18.

[29] A. Cornish-Bowden, Fundamentals of Enzyme Kinetics., Portland Press., 2004.

[30] T. Schulmeister, Mathematical modelling of the dynamic behaviour of amperometric enzyme electrodes., Selective Electrode Rev. 12 (1990) 203–260.

[31] W. Blaedel, R. Boguslaski, A chemical amplification in analysis., a review. Anal. Chem. 50 (1978) 1026–1033.

[32] J. Kulys, Development of new analytical systems based on biocatalysts., Enzyme and Microbial Technology. 3 (1981) 344–352.

[33] E. Gaidamauskait, R. Baronas, A Comparison of Finite Difference Schemes for Computational Modelling of Biosensors Nonlinear Analysis., Modelling and Control. 12 ((3)) (2007) 359–369.

[34] H. Mehrer, Diffusion in solids., Springer Berlin. (2007) 40–50.

[35] J. Crank, The Mathematics of Diffusion., Oxford University Press., 2nd edition edn., 1975.

[36] S. De Groot, P. Mazur, Thermodynamics of Irreversible Processes., NorthHolland Publ. Comp. .

[37] L. Mejlbro, The complete solution of Fick's second law of diffusion with time-dependent diffusion coefficient and surface concentration., Technical University of Denmark., 1996.